Modulation of Tropical Cyclogenesis Location and Frequency over the Indo–Western North Pacific by the Intraseasonal Indo–Western Pacific Convection Oscillation during the Boreal Extended Summer

QIUYUN WANG

College of Global Change and Earth System Sciences, Beijing Normal University, Beijing, China

JIANPING LI

State Key Laboratory of Earth Surface Processes and Resource Ecology, and College of Global Change and Earth System Sciences, Beijing Normal University, Beijing, and Laboratory for Regional Oceanography and Numerical Modeling, Qingdao National Laboratory for Marine Science and Technology, Qingdao, China

YANJIE LI

State Key Laboratory of Numerical Modeling for Atmospheric Sciences and Geophysical Fluid Dynamics (LASG), Institute of Atmospheric Physics, Chinese Academy of Sciences, Beijing, China

JINGWEN ZHANG

Chengdu Meteorological Bureau, Chengdu, China

JIAYU ZHENG

State Key Laboratory of Tropical Oceanography, South China Sea Institute of Oceanology, Chinese Academy of Sciences, Guangzhou, China

(Manuscript received 10 February 2017, in final form 27 October 2017)

ABSTRACT

The influence of the intraseasonal Indo–western Pacific convection oscillation (IPCO) on tropical cyclone (TC) genesis location and frequency over the Indo–western North Pacific (WNP) during the boreal extended summer (May–October) is explored. Observational analysis shows that the impacts of the intraseasonal IPCO on TCs over the Indo–WNP include an evident ''phase lock of TC genesis location'' and distinct differences in TC frequency. In the WNP, in the positive intraseasonal IPCO phase, the atmosphere gains heat through the release of latent heat in cumulus convective condensation, and the anomalous cyclonic circulation weakens the western Pacific subtropical high (WPSH) and enhances TC genesis, thereby tending to produce many more TCs. Moreover, the diminished WPSH and the westward shift of the centers of anomalous cyclonic circulations lock TC genesis locations to the west WNP and lower latitudes (around 5°–20°N), especially in the South China Sea. The almost opposite situation occurs in a negative phase. In the north Indian Ocean, the total TC genesis frequencies in the two intraseasonal IPCO phases are approximate. However, in the positive intraseasonal IPCO phase, the environmental conditions to the north of 13°N are similar to those in the WNP except without the WPSH control, whereas south of 13°N the situation is reversed, leading to a northward shift of the TC genesis location (around 13°–20°N). The negative phase reflects an opposite situation.

1. Introduction

Tropical cyclones (TCs), also widely known as typhoons in the western North Pacific (WNP), cyclones in the Indian Ocean, or hurricanes in the Atlantic, are some of the most damaging weather events in the world (Li et al. 2016a). On the one hand, they cause enormous damage to the local residents and their livelihood, but on the other hand many countries depend on TC precipitation for their domestic and agricultural water supplies (Elsberry and Tsai 2016). Numerous studies have demonstrated that SST variability has an important

Corresponding author: Dr. Jianping Li, ljp@bnu.edu.cn

DOI: 10.1175/JCLI-D-17-0085.1

effect on TC activity on interdecadal as well as other time scales (Gray 1968; Yumoto and Matsuura 2001; Emanuel 2003, 2005; Webster et al. 2005; Liu and Chan 2008; Knutson et al. 2010; Chan 2000; Wang and Chan 2002; Sobel and Camargo 2005; Camargo et al. 2007; Kim et al. 2009; Zhan et al. 2011a,b, 2014, 2016, 2017; Huo et al. 2015; Yu et al. 2016). On interannual time scales, TC activity can also be modulated by cross-equatorial flow (Li 1956; Feng et al. 2014), the stratospheric quasi-biennial oscillation (QBO) (Chan 1995; Camargo and Sobel 2010), and cross-basin SST gradient (Kossin and Vimont 2007; Zhan et al. 2013; Zhao et al. 2016). On intraseasonal time scales, previous research (Hartmann and Maloney 2001; Zhu et al. 2004; Kim et al. 2008; Huang et al. 2011; Li and Zhou 2013a,b; Wang and Moon 2017) has suggested that TC activity is modulated by the tropical 30–60-day intraseasonal oscillation (ISO), also known as the Madden–Julian oscillation (MJO), showing significant subseasonal variation (Madden and Julian 1972, 1994; Madden 1986).

The tropical Indo–western Pacific is the key area of the 30–60-day ISO, and the TC genesis frequency over the Indo–WNP is 36% of the global total (Li et al. 2016b). Research has been increasingly focused on the relationship between TCs and the ISO in this area. Hartmann and Maloney (2001) used a barotropic energy conversion perspective to show that the MJO affected tropical cyclogenesis in the North Pacific Ocean during Northern Hemisphere summer. Zhu et al. (2004) investigated the fact that tropical depressions (TDs) and TCs formed more readily in the wet phase of the MJO over the Indo–western Pacific from September 1996 to June 1997.

Convection plays an important role in the relationship between TCs and the ISO, and tropical convection exhibits a prominent ISO. Lau and Chan (1986) pointed out that a dipole convection pattern linked the Indian Ocean and the western Pacific during summertime (May–October) from 1975 to 1982 (except 1978). Zhu and Wang (1993) further investigated the convection seesaw events over the equatorial eastern Indian Ocean (EEIO) and the WNP case by case for 1981–85 and suggested that the seesaw formation was associated with interactions between propagating low-frequency convection systems and the summer monsoon circulation. Y. J. Li et al. (2013) found that this out-of-phase fluctuation of convection anomalies over the Indo–western Pacific was also evident at the interannual scale during the boreal summer from 1979 to 2010, with dipole centers located over the north Indian Ocean [NIO; the Arabian Sea (ARB) and the south of the Bay of Bengal (BOB)] and the WNP regions. They defined these out-of-phase convection anomalies over the Indo–western Pacific as the Indo–western Pacific convection oscillation (IPCO) (Y. J. Li et al. 2013) and found that the IPCO exhibited a quasi-biennial variability in boreal summer and was strongly associated with the East Asian summer monsoon. Previous studies have demonstrated that the IPCO has significant intraseasonal variations (Zhang et al. 2015), and the average locations of the convection centers of the intraseasonal IPCO change slightly and lie over the EEIO (5°S–10°N, 70°–100°E) and the WNP (5°–20°N, 110°–160°E), respectively. The intraseasonal IPCO is divided into propagating and nonpropagating parts. During the boreal extended summer, the propagation of the boreal summer ISO (BSISO) (Kikuchi et al. 2012) has a close connection with propagating part of the intraseasonal IPCO. The propagating part related to the BSISO can explain less than 40% of the intraseasonal IPCO. The intraseasonal IPCO is an important link in weather and climate events between the Indian Ocean and WNP (J. P. Li et al. 2013a), which has a closed associated with the Indian–Asia–Pacific (IAP) teleconnection, the East Asia–Pacific (EAP) teleconnection, or the Pacific–Japan (PJ) teleconnection. However, to the authors' knowledge, there is no published study on the relationship between TC activity over the Indo–WNP and the intraseasonal IPCO. What is their relationship? And what supports this relationship? These questions are the motivation for the present study. Our primary concern in this paper is to show the influence of the intraseasonal IPCO on the location and frequency of TC genesis based on the perspective of the Indo–WNP basin.

The paper is organized as follows. In section 2, we provide a brief review of the data and methodologies in the analyses. Section 3 shows the statistical characteristics of the location and frequency of TC genesis in the positive and negative intraseasonal IPCO phases, and section 4 discusses possible physical mechanisms to explain the differences in the location and frequency of TC genesis in the different intraseasonal IPCO phases. Section 5 depicts an assessment to TC genesis and environmental conditions of TC genesis by means of the GPI. Section 6 presents a summary of the key results and conclusions.

2. Data and methodology

a. Data

Daily datasets for the 6-month boreal extended summer (May–October) in the 37 years from 1979 to 2015 are analyzed. These consist of interpolated outgoing longwave radiation (OLR) data (Liebmann and Smith 1996) and National Centers for Environmental Prediction (NCEP)–National Center for Atmospheric Research (NCAR) reanalysis data (Kalnay et al. 1996), including horizontal wind fields, vertical velocity, geopotential height, relative humidity, and surface heat flux

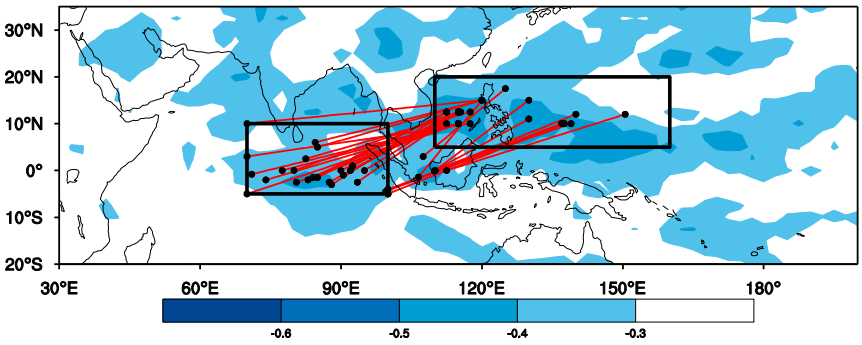

FIG. 1. Teleconnectivity map of the boreal extended summer OLR anomalies over the Indo–western North Pacific for the period 1979–2015. Only regions with negative correlation coefficients less than −0.3 are shaded (above the 99% confidence level). Each red line connects two selected points (black dots) with the strongest negative correlation on the one-point correlation map. The two black rectangles denote the selected regions WNP (5°–20°N, 110°–160°E) and EEIO (5°S–10°N, 70°–100°E).

data, all on 2.5° × 2.5° global grids except the surface heat flux dataset, which is on a Gaussian grid of spectral T62 resolution with 192 × 94 grid points.

Historical records of TC activity over the WNP are obtained from the Regional Specialized Meteorological Center (RSMC) best-track data (available online at http://www.jma.go.jp/jma/jma-eng/jma-center/rsmc-hp-pub-eg/trackarchives.html) of the JMA (Japan Meteorological Agency). And that over the NIO were obtained from the International Best Track Archive for Climate Stewardship (IBTrACS; available online at https://www.ncdc.noaa.gov/ibtracs/) from the National Oceanic and Atmospheric Administration (NOAA). Only TCs that reach tropical storm intensity (maximum sustained 10-m wind speed $\geq 17.2\,\mathrm{m\,s^{-1}}$) in the period 1979–2015 are considered in our analysis.

b. Statistical methods

We apply a 30–60-day Lanczos bandpass filter using 139 weights to anomalies of the aforementioned meteorological elements, except the TC data. Note that we use the period 1979–2015 for all data unless otherwise stated. An IPCO index has been defined by Y. J. Li et al. (2013) as

$$\mathrm{IPCOI} = \mathrm{OLR}_{\mathrm{NIO}} - \mathrm{OLR}_{\mathrm{WNP}}, \tag{1}$$

where $\mathrm{OLR}_{\mathrm{NIO}}$ and $\mathrm{OLR}_{\mathrm{WNP}}$ are the normalized area-averaged time series of OLR anomalies over the NIO and WNP, respectively. Equation (1) is also used for the intraseasonal IPCO [for WNP (5°–20°N, 110°–160°E) and NIO (5°S–10°N, 70°–100°E)] but with a 30–60-day bandpass filter applied to the area-averaged OLR anomalies. A value of IPCOI greater than 1 is used to define a positive phase of the IPCO, while an IPCOI value less than −1 defines the negative phase, and the neutral phase is defined when the absolute value of IPCOI is less than or equal to 1.

The intraseasonal IPCO is examined over a longer time series than in previous studies (figure not shown). Teleconnection and regression analysis are employed in our study in order to further verify the intraseasonal IPCO (Figs. 1 and 2). The statistical significance of the correlation between two autocorrelated time series is assessed via the two-tailed Student's t test using the effective number of degrees of freedom N^{eff}, which can be given by the following approximation (Pyper and Peterman 1998; Li et al. 2012; J. P. Li et al. 2013b; Xie et al. 2014; Sun et al. 2015):

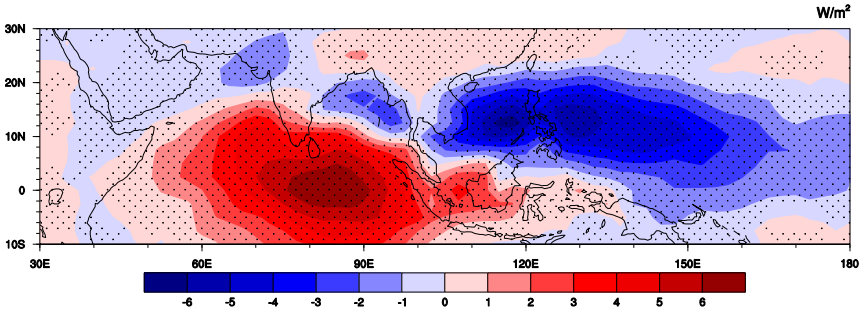

FIG. 2. Regression of the intraseasonal IPCO onto OLR anomalies (shading; $\mathrm{W\,m^{-2}}$). The stippled regions denote significance at the 99% confidence level using the Student's t test.

$$\frac{1}{N^{\text{eff}}} \approx \frac{1}{N} + \frac{2}{N}\sum_{j=1}^{N}\frac{N-j}{N}\rho_{XX}(j)\rho_{YY}(j), \qquad (2)$$

where N is the sample size and $\rho_{XX}(j)$ and $\rho_{YY}(j)$ are the autocorrelations of the two sampled time series X and Y at time lag j, respectively.

Composite analysis and an improved Gill model (Xing et al. 2014) are employed to explore possible physical mechanisms. The Gill model response is calculated for asymmetric heating and cooling sources positioned at the dipole centers. We divide the NIO into two in the latitudinal direction along 13°N according to the first EOF mode of daily OLR anomalies, and the NIO basin is also split into the ARB and the BOB along 76°E.

c. *Genesis potential index*

To further verify the robustness of our results, 30–60-day bandpass-filtered genesis potential index (GPI) anomalies are employed in this paper. The GPI is developed by Emanuel and Nolan (2004) was motivated by the work of Gray (1979). Previous researches have proven that the GPI is able to replicate the observed climatological annual cycle, interannual variations of TC genesis in several different basins, and global TC genesis on intraseasonal time scales (Camargo et al. 2007, 2009; Jiang et al. 2012; Zhao et al. 2015a,b). The GPI is defined as

$$\text{GPI} = |10^5\eta|^{3/2}\left(\frac{\mathcal{H}}{50}\right)^3\left(\frac{V_{\text{pot}}}{70}\right)^3(1+0.1V_{\text{shear}})^{-2}, \qquad (3)$$

where η is the absolute vorticity at 850 hPa (s^{-1}), $\mathcal{H}$ is the relative humidity at 600 hPa (%), V_{shear} is the magnitude of the vertical wind shear between 850 and 200 hPa ($m\,s^{-1}$), and V_{pot} is the potential intensity ($m\,s^{-1}$) (Emanuel 1995; Bister and Emanuel 2002a,b). Moreover, according to the method of Jiang et al. (2012), the importance of each component of the GPI is assessed. In their work, the GPI anomalies associated with the ISO GPI^{ISO} were decomposed:

$$\begin{aligned}\text{GPI}^{\text{ISO}} = {} & \overline{r}\,\overline{\psi}\,\overline{s}\,\eta^{\text{ISO}} + \overline{\eta}\,\overline{\psi}\,\overline{s}\,r^{\text{ISO}} + \overline{r}\,\overline{\eta}\,\overline{s}\,\psi^{\text{ISO}} + \overline{r}\,\overline{\psi}\,\overline{\eta}\,s^{\text{ISO}} \\ & + [\overline{\psi}\,\overline{s}(r'\eta')^{\text{ISO}} + \overline{r}\,\overline{s}(\psi'\eta')^{\text{ISO}} + \cdots + \overline{r}(s'\psi'\eta')^{\text{ISO}} \\ & + \cdots + (r's'\psi'\eta')^{\text{ISO}}],\end{aligned} \qquad (4)$$

where the terms r, s, ψ, and η indicate the GPI components associated with 600-hPa relative humidity, with vertical wind shear, with potential intensity, and with 850-hPa absolute vorticity, respectively. An overbar denotes a climatological annual cycle component, and the prime denotes a fluctuation. The total GPI^{ISO} can be decomposed into the sum of four linear terms, which are associated with the ISO of each of the four factors, while the other three terms remain constant at their mean values. Moreover, the contributions of nonlinear terms can also be examined by higher-order variances of two or more of the four factors [total 11 terms included within square brackets in Eq. (4)].

TABLE 1. The total number of TCs and mean and standard deviation of meridional and zonal locations of tropical cyclogenesis over the WNP in boreal extended summer in the positive and negative intraseasonal IPCO phases (1979–2015). Two asterisks indicate significance at the 99% confidence level using the Student's t test.

WNP		IPCO+	IPCO−
Total No.		294	136
Meridional	Mean	14.34°N**	16.00°N**
	Std dev	4.98°	5.50°
Zonal	Mean	138.10°E**	143.13°E**
	Std dev	14.93°	14°

3. TC genesis location and frequency in the positive and negative intraseasonal IPCO phases

The TC genesis location and frequency change with the phases of the intraseasonal IPCO over the Indo–WNP in the boreal extended summer. In the WNP, there are significant differences in total number (as shown in Table 1) and frequency of TCs formed in the different intraseasonal IPCO phases. Figure 3 shows that there tend to be many more TCs in the WNP during the positive phase of the intraseasonal IPCO (over twice as many as in the negative phase; see Table 1), especially in the South China Sea (SCS). The TC genesis locations are clustered together, while the reverse is true in the negative intraseasonal IPCO phase. In the NIO, there are no significant differences in total number (as shown in Table 2) and frequency of TCs formed in the different intraseasonal IPCO phases, and the TC genesis locations are more clustered in the positive intraseasonal IPCO phase, as in the WNP, but tend to be more dispersed in the negative phase. Furthermore, it is obvious that there is only one TC genesis at the average locations of the convection centers over the Indian Ocean in the positive phase, and about 41% of TCs occur over there in the negative phase. To further reveal the distribution of the TC genesis locations, we examined the meridional and zonal distributions separately.

In the WNP, the meridional distribution (Fig. 4a) of the TC genesis locations shifts southward in the intraseasonal IPCO positive phase compared with the negative phase [the average latitude of the distribution is farther south (Table 1), and the distribution range changes from 5.3°–30°N to 4°–28.5°N], and the TC genesis locations are distributed mainly over 5°–20°N (roughly 84.7% vs 73.5%

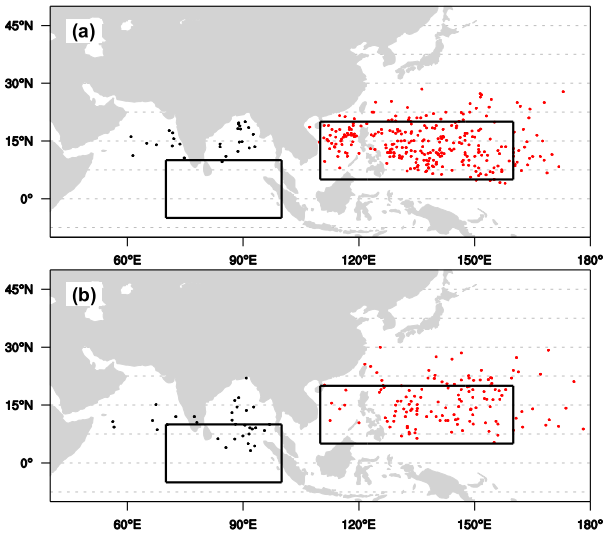

FIG. 3. TC genesis location (tiny dots, red and black denote TCs over the WNP and NIO, respectively) during the (a) positive and (b) negative intraseasonal IPCO phases over the Indo–WNP in the boreal extended summer for the period 1979–2015. The gray dashed lines denote latitude lines at 7.5° intervals. The two black rectangles are same as in Fig. 1.

in the negative phase). In the zonal distribution (Fig. 4b), there is no significant difference in concentrative degree (the standard deviation is similar) associated with the Philippines, but the frequency of TC genesis increases remarkably in the SCS in the intraseasonal IPCO positive phase, reaching 7.14 times the frequency in the negative phase. The TC genesis region shifts to the west of the WNP (the average longitude of the distribution shifts about 5° westward, and the distribution range changes from 111.1°–178.1°E to 107.2°–172.9°E). In the WNP, the average location in the positive (negative) intraseasonal IPCO phase is similar to the wet (dry) BSISO phase

TABLE 2. As in Table 1, but over the NIO. Two asterisks indicate significance at the 99% confidence level using the Student's *t* test.

NIO		IPCO+	IPCO−
Total No.		27	32
Meridional	Mean	15.22°N**	10.3°N**
	Std dev	2.96°	4.08°
Zonal	Mean	81.41°E	84°E
	Std dev	10.43°	11.21°

(Fig. 3 in Yoshida et al. 2014), which locates in the southern and eastern (northern and western) portions of the WNP. These features imply that there is a close association between the BSISO and propagating part of the intraseasonal IPCO. But in their study, they focused on the differences in favorable phases of the BSISO for TC genesis among the five synoptic-scale flow patterns (including a shear line, a confluence region, an easterly wave, a monsoon gyre, and a preexisting tropical cyclone) and did not indicate detailed features of the distribution of TC genesis. The similarities not only verify the previous work but also further demonstrate the present results' reliability. In the NIO, the total TC genesis frequencies in the positive and negative intraseasonal IPCO phases are similar, which is different from previous study (Kikuchi and Wang 2010). Also, the effects of the intraseasonal IPCO on TC genesis in each phase are different than that of the BSISO. This difference can better verify that the intraseasonal IPCO is not essentially the same as the BSISO. In the meridional distribution (Fig. 5a), TC genesis can be observed over a range extending around 10.41° poleward of 9.59°N in the positive intraseasonal IPCO phase, with locations mainly from 13° to 20°N and distributed rather closely (standard deviation is 2.96° vs 4.08° in the negative phase; Table 2). However,

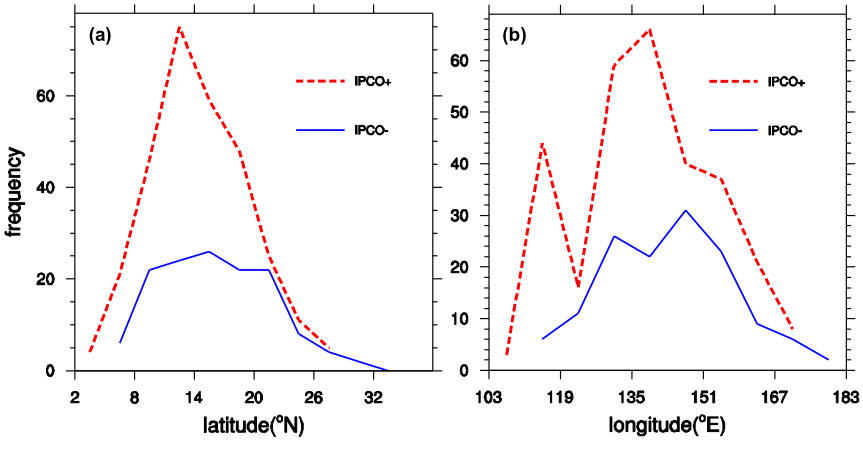

FIG. 4. (a) Meridional and (b) zonal distributions of TC genesis frequency in the positive (red dotted line) and negative (blue solid line) intraseasonal IPCO phases over the WNP in boreal extended summer for the period 1979–2015.

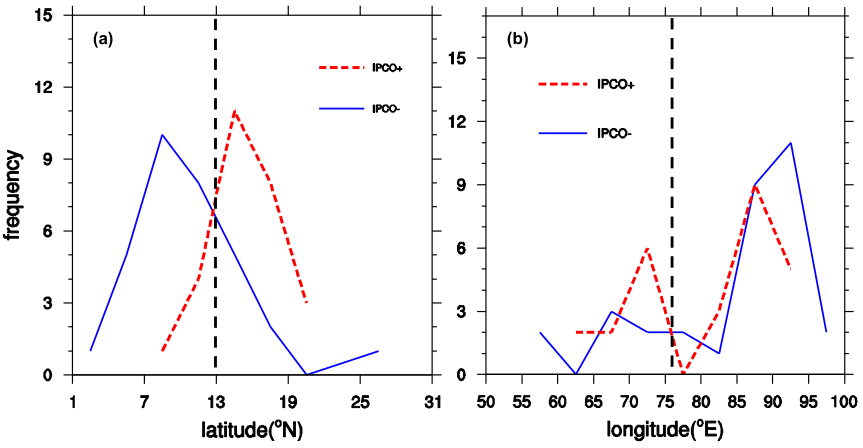

FIG. 5. As in Fig. 4, but for the NIO. The black dashed lines denote the lines of the meridional and zonal demarcations in (a) and (b), respectively.

in the negative phase, TC genesis occurs widely, from 3.2°N at least as far poleward as 22°N and the TC genesis locations tend to be more dispersed. In the zonal distribution (Fig. 5b), the TCs form closer to the Indian subcontinent in the positive intraseasonal IPCO phase, particularly in the ARB. In the negative phase, the opposite holds, with TCs forming over a wider zonal range extending to 56.2°–96.8°E compared with a range of 60.9°–93°E in the positive phase. We use the phrase "phase lock of TC genesis location" to describe the more concentrated distribution of TC genesis locations over the Indo–WNP in the positive intraseasonal IPCO phase and the wider dispersion in the negative phase.

4. Possible physical mechanisms

As discussed above, in the WNP, TC genesis is favored in the positive intraseasonal IPCO phase, especially in the SCS. More TCs generate in the west of the WNP and at lower latitudes (around 5°–20°N). Fewer TCs form and the distribution of the TC genesis locations is more dispersed in the negative phase. In the NIO, there is little difference in the total number of TCs generated between the positive and negative intraseasonal IPCO phases. When the intraseasonal IPCO is in a positive phase, TC genesis mainly occurs over 13°–20°N and closer to the Indian subcontinent than in the negative phase, particularly in the ARB. In contrast, the distribution tends to be more dispersed in the negative phase. In an attempt to explain this phase lock of TC genesis location and the distinct differences in TC frequency between the positive and negative intraseasonal IPCO phases over the Indo–WNP, we present possible physical mechanisms, including the thermodynamic effect of relative humidity in the middle atmosphere and circulation conditions.

a. Thermodynamic effect of relative humidity in the middle atmosphere

The energy can be provided for TC genesis through latent heat release of cumulus convective condensation. Through simplifying the equations of motion, the relationship between radial temperature gradient $\partial T_v/\partial r$ and vertical tangential wind shear $\partial v/\partial \log p$ can be obtained (Anthes 1982, Holland 1987, Zhu et al. 2007, Kepert 2010):

$$\frac{\partial v}{\partial \log p}\left(f+\frac{2v}{r}\right)=-R_d\frac{\partial T_v}{\partial r}, \tag{5}$$

where v is the tangential velocity ($v>0$ represents cyclonic flow), r is radial distance to the TC center, f is the Coriolis parameter, p is pressure, R_d is the gas constant for dry air, and T_v is virtual temperature. Equation (5) shows that the TC warm-core structure favors weakening of the TC circulation with height, which implies that the warm-core structure plays a vital role in TC genesis. The cumulus convective condensation heating contributes to the development of the warm core. Furthermore, to some extent, relative humidity represents the available latent heat of condensation. Figure 6 illustrates the composite difference between positive and negative phases of relative humidity anomalies at the 600-hPa level in the boreal extended summer, representing the water vapor conditions in the middle atmosphere. Positive values indicate that there tends to be more water vapor in the intraseasonal IPCO positive phase than in the negative phase. It is well known that the strongest convective activity occurs in the middle atmosphere (corresponding to heights from about 3–7 or 8 km), and as we are considering tropical cyclogenesis, we analyze the relative humidity at the 600-hPa level combined with

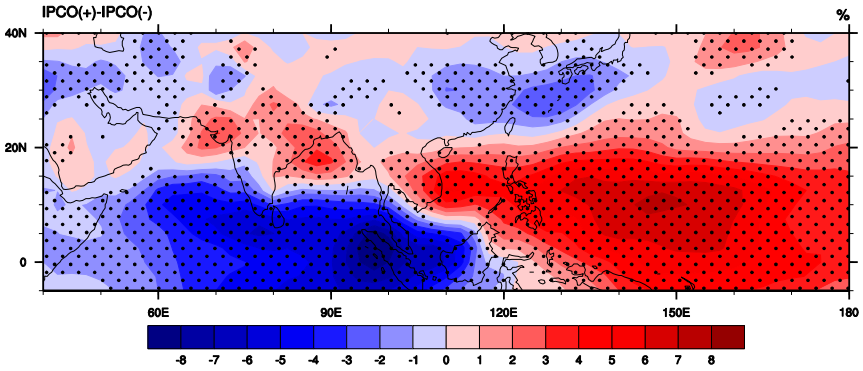

FIG. 6. Composite difference in the relative humidity anomalies (%) at the 600-hPa level between the positive and negative intraseasonal IPCO phases over the Indo–WNP in the boreal extended summer for the period 1979–2015. The stippled regions denote significance at the 99% confidence level using the Student's *t* test.

the previous studies (Gray 1979; Wang and Moon 2017). In the WNP, Fig. 6 shows that the maximum relative humidity anomalies are found from the east of the Philippines to around 15°N, 160°E, and also in the SCS, indicating that there might be more water vapor in these regions in the intraseasonal IPCO positive phase than in the negative phase. In other words, the release of more convective condensation latent heat favors the conversion into perturbation potential energy (PPE), favoring the development and persistence of the TC warm core structure and thereby leading to more TCs generating in the positive intraseasonal IPCO phase. Low values of relative humidity anomalies are centered in the WNP north of 25°N, which means the release of less convective condensation latent heat, thereby suppressing the development and persistence of the TC warm core structure. Consequently, there is less TC genesis there. These features result in a southward shift of TC genesis over the WNP in the positive phase. In fact, high water vapor concentrations exist in the neighborhood of the equator, but there is no TC genesis because of the small Coriolis parameter. The opposite situation holds for the negative phase. Low values of relative humidity anomalies are centered in the WNP south of 25°N, which suppress the TC genesis in this region, thereby leading to a more dispersed distribution in the negative phase. In the NIO, in the positive phase of the intraseasonal IPCO, owing to the low relative humidity anomalies, low TC genesis rates are centered on the western flank of Indonesia and high values next to the Indian subcontinent, which leads to a northward shift of TC genesis locations relative to those seen in the negative phase, restricting the TC genesis locations mainly between 13° and 20°N, and rather close to the Indian subcontinent. In the negative phase, the opposite situation occurs. The asymmetry of the relative humidity north and south of 13°N in the NIO results in an approximate total number of TCs being formed in the two phases.

b. Circulation conditions

An initial perturbation is essential for TC genesis, but an air parcel must undergo a considerable amount of forced ascent before it reaches the level of free convection in the unsaturated mean tropical atmosphere (Holton 2004). As a result, suitable circulation conditions are important, including low-level vorticity, convergence, vertical velocity, and wind field, and the western Pacific subtropical high (WPSH) cannot be ignored as a crucial impact factor in the WNP. Elsberry et al. (1987) summarized the impact of low-level vorticity on TC genesis in terms of two mechanisms. One involves the interactions between heating and rotation, when the atmosphere is heated on a scale smaller than the deformation radius. This results in low-level convergence, updraft, and upper-level divergence. The Rossby deformation radius R_D is defined by

$$R_D = \frac{NH_0}{(f+\zeta)^{1/2}\left(\frac{2v}{r}+f\right)^{1/2}}, \tag{6}$$

where N is the Brunt–Väisälä frequency, ζ is the relative vorticity, f is the Coriolis parameter, H_0 is the scale height, v is the tangential velocity, and r is radius of curvature. Equation (6) shows that R_D decreases with increasing vorticity, which reduces the scale of the responses and increases the efficiency of conversion from latent heat release to rotational motion (Hack and Schubert 1986).

Figure 7 is equivalent to Fig. 6, but for the vorticity and divergence anomalies at the 850-hPa level and vertical *p*-velocity anomalies at the 500-hPa level. In the positive intraseasonal IPCO phase, there is higher

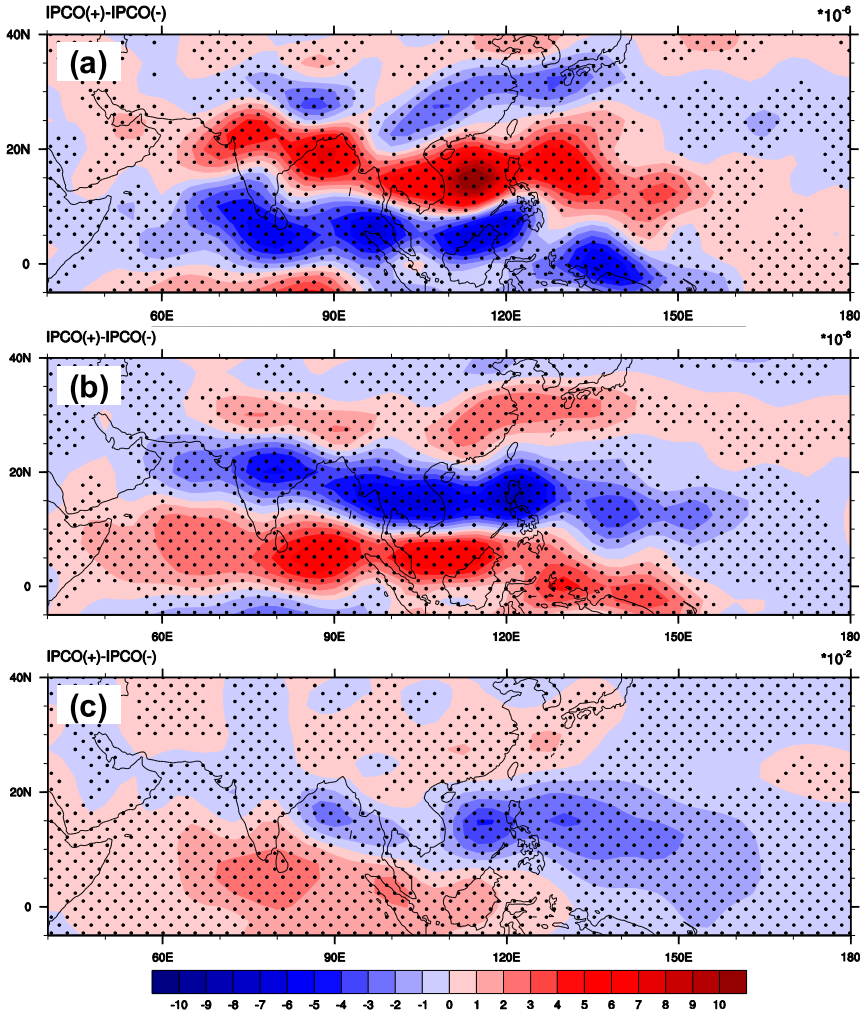

FIG. 7. As in Fig. 6, but for the (a) vorticity and (b) divergence anomalies (s^{-1}) at the 850-hPa level and (c) vertical p-velocity anomalies ($Pa\,s^{-1}$) at the 500-hPa level.

vorticity than in the negative phase over a region 15° poleward of 10°N over the Indo–WNP, especially in the SCS and north of 13°N in the NIO (Fig. 7a), which gives lower R_D in these areas, resulting in a reduction in the scale of the responses. More convective condensation may increase PPE in these regions, and the lower RD leads to the increased conversion efficiency from PPE to kinetic energy (KE) of rotational motion in these areas, enhancing TC genesis in the positive phase. Meanwhile, convergent lower airflows are stronger in the positive than in the negative phase in the north of the NIO and around 15° equatorward of 20°N in the WNP (Fig. 7b), leading to ascending motion in these regions. As shown in Fig. 7c, vertical p velocity is negative at the 500-hPa level about 15° equatorward of 20°N in the WNP, which implies larger upward vertical velocity in the positive intraseasonal IPCO phase than in the negative phase. This is crucial for heat transfer from the lower atmosphere to the upper atmosphere, which contributes to the development and persistence of the TC warm core structure through the aforementioned latent heat release in the middle atmosphere. Strongly negative values of vertical p velocity are located on both sides of the Philippines and in the north of the BOB. These conditions support TC genesis in these regions in the positive phase.

Corresponding to stronger updrafts and the cyclonic vorticity source mentioned above, there is a strongly anomalous cyclonic circulation at low latitudes in the WNP when the intraseasonal IPCO is in a positive phase (Fig. 8a). This is another reason why TCs tend to develop in this phase, and might explain why TCs also occur more readily north of 13°N in the NIO when the intraseasonal IPCO is in a positive phase. The reverse is true in the negative phase (Fig. 8b); anomalous anticyclonic circulation appears over the WNP and north of

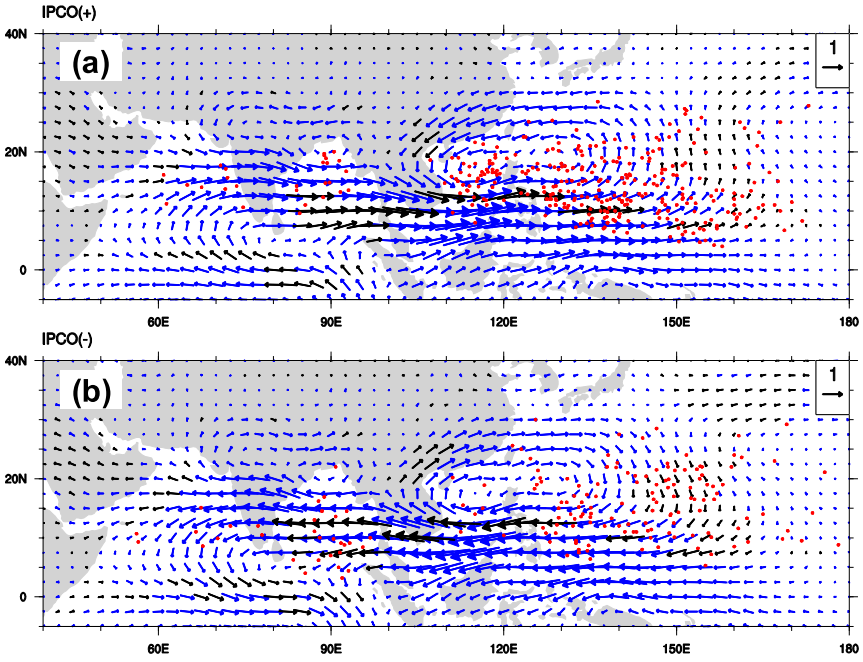

FIG. 8. (a) Composite map of the horizontal wind anomalies (vectors; m s^{-1}) at 850 hPa over the Indo–WNP in the boreal extended summer for the period 1979–2015 for the positive intraseasonal IPCO phase. The red dots indicate the locations of tropical cyclogenesis, and blue vectors show significance at the 99% confidence level. (b) As in (a), but for the negative intraseasonal IPCO phase.

13°N in the NIO, suppressing TC genesis. In contrast, tropical cyclogenesis is enhanced at some latitudes equatorward of 13°N in the NIO, leading to a wider spread over the NIO. The asymmetric anomalous circulations in the NIO north and south of 13°N give similar total numbers of TC genesis in the two phases. In addition, more evidence for the anomalous circulation at low latitudes can be found from the Gill model response of horizontal wind and pressure to symmetric heating and cooling sources in the lower layer in the positive and negative intraseasonal IPCO phases (Fig. 9).

Aside from this direct effect of anomalous circulation at low latitudes on TC genesis, another effect is through changing the WPSH in the WNP. The WPSH, a large-scale anticyclonic circulation located over the subtropical Pacific throughout the year, has an important influence on both adjacent regions and on the global circulation (Lu 2001; Li et al. 2011), and indeed on TC activity (Ho et al. 2004; Zhu et al. 2007). In Fig. 10, there is a significant difference in the WPSH position between the positive and negative intraseasonal IPCO phases west of 160°E in the WNP, which is consistent with the location of the intraseasonal IPCO convection center in the WNP, further supporting the effect of the intraseasonal IPCO on the WPSH. When the intraseasonal IPCO is in a negative phase, the WPSH is abnormally intensified with a strongly anomalous anticyclonic circulation at low latitudes. The western edge of the 1520-gpm surface leans farther to the west and the ridge is farther to the south than normal, which results in drier conditions than normal, further suppressing TC genesis over the WNP. However, when the intraseasonal IPCO is in a positive phase, a strongly anomalous cyclonic circulation at low latitudes weakens and shrinks the WPSH, and the ridge moves farther to the north than normal. These changes in the WPSH favor tropical cyclogenesis and lock the sites of TC genesis, so that there tend to be more TCs at lower latitudes and farther west in the WNP than in the negative phase.

5. Assessment to TC genesis and environmental conditions of TC genesis by means of GPI at two phases

The aforementioned above give a qualitative assessment to TC genesis; to further verify our results, the GPI (Camargo et al. 2007, 2009) is employed. As can be seen from Fig. 11a, when the intraseasonal IPCO is in its positive phase, there are positive anomalies of the GPI compared with the negative phase from 10° to 20°N over the WNP, especially on both sides of the Philippines. This means that more TCs generate in these regions. A

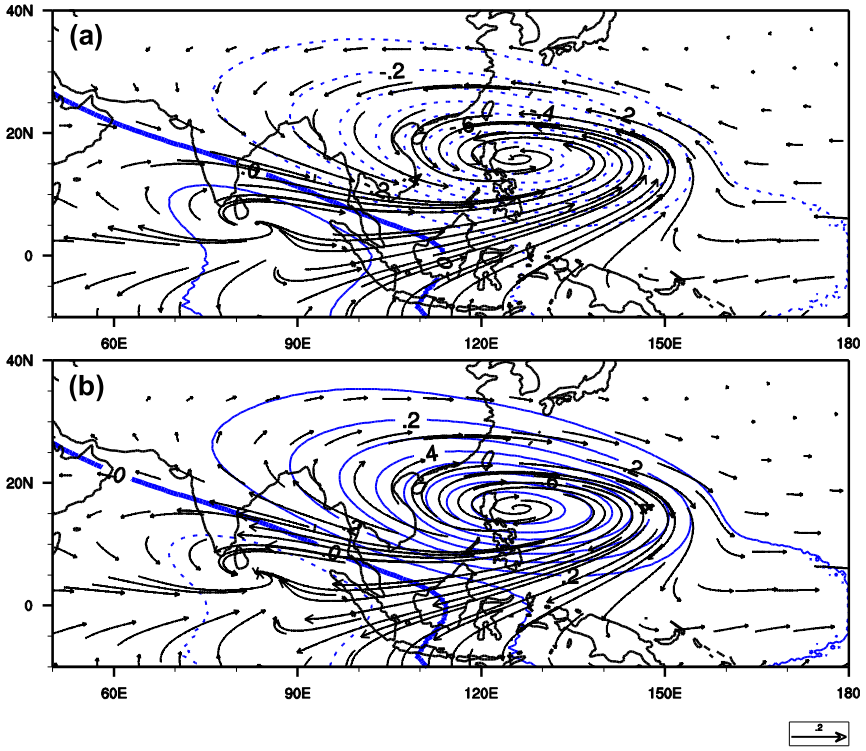

FIG. 9. (a) As in Fig. 8a, but for the Gill model response of horizontal wind (streamlines) and pressure (blue contours; hPa) in the lower layer. Blue solid (dashed) contours indicate positive (negative) pressure, contour interval is 0.1 hPa, and the thick solid line is the zero contour. (b) As in (a), but for the negative intraseasonal IPCO phase.

similar situation exists in the NIO north of 13°N, particularly near the Indian subcontinent. In contrast, when the intraseasonal IPCO is in its negative phase, positive anomalies of GPI occur in the NIO south of 13°N and the SCS south of 10°N, and so TCs form more easily in these regions. These results are similar to the aforementioned analyses except for fine distinctions, such as the westward distribution of TCs over the WNP.

Moreover, following the method of Jiang et al. (2012), the contribution of the total linear terms of the GPI (Fig. 11b), total nonlinear terms of the GPI (Fig. 11c), and each linear term (which are associated with the ISO of each of the four factors, low-level vorticity, midlevel relative humidity, vertical wind shear, and potential intensity; Fig. 12) of the GPI are assessed. As can be seen from Fig. 11b, we find that the whole pattern of total linear terms is similar to the GPI anomalies, except that the center position of the total linear term is farther south than those of the GPI over the Indo–WNP. The total contribution of linear terms can better express the westward distribution over the WNP than the GPI, and it is more consistent with actual distribution over the NIO. The total contribution of nonlinear terms of GPI shows an opposite pattern with GPI anomalies at corresponding phases in most regions, except for the SCS south of 10°N, which means that the nonlinear terms of the GPI play different roles in different basins. On the one hand, the total nonlinear terms of the GPI have no significant contribution over the NIO. On the other hand, it cannot be ignored that nonlinear terms of

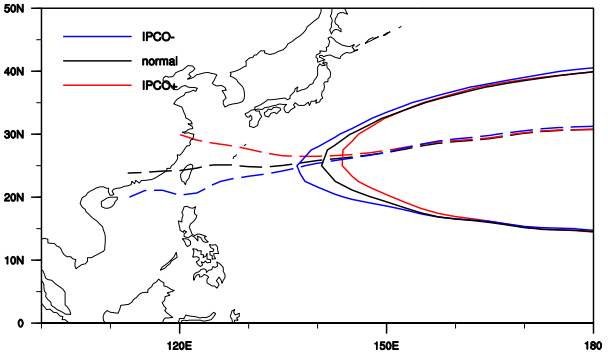

FIG. 10. The ridge and extent of 850-hPa level WPSH in boreal extended summer for 1979–2015. The black, red, and blue lines are for the climatological mean and the positive and negative intraseasonal IPCO phases, respectively. Dashed lines indicate the WPSH ridge, and solid lines the 1520-gpm isoline of 850-hPa geopotential height.

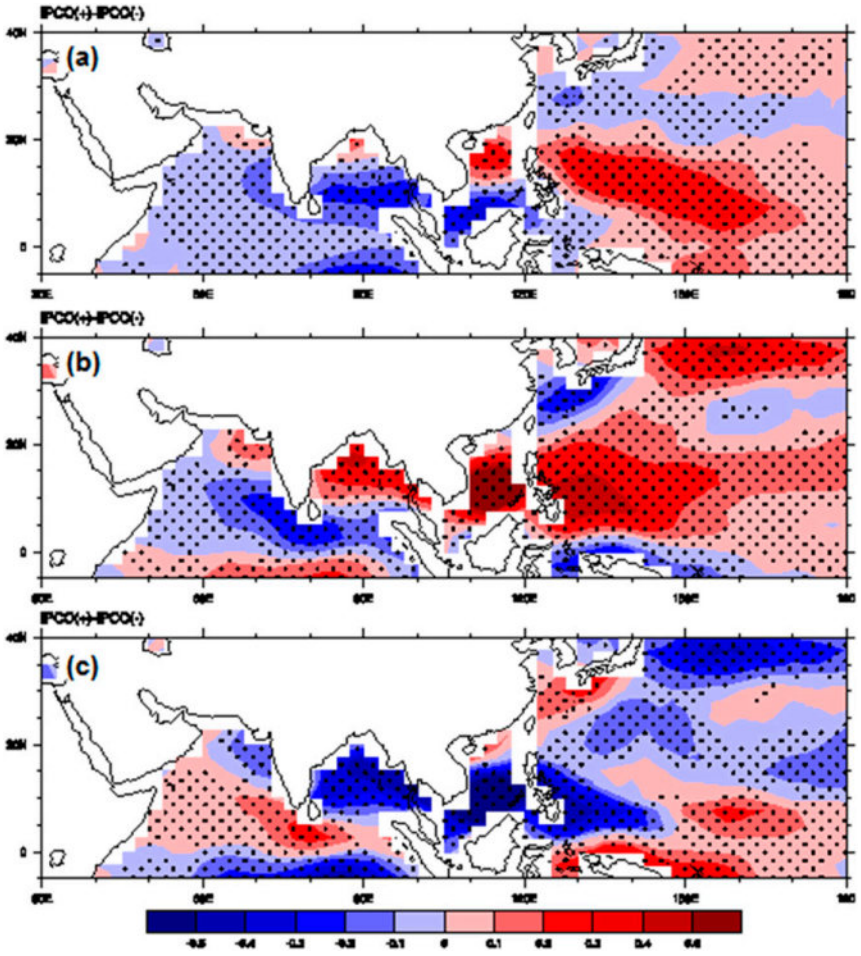

FIG. 11. As in Fig. 6, but for the (a) GPI anomalies, (b) total contribution from the four linear terms, and (c) total contribution from nonlinear terms of GPI.

GPI play an important role in modulating the center position of total contribution of linear terms. As can be seen from Fig. 12, it is obvious that the patterns of linear terms associated with the ISO of the 850-hPa vorticity (Fig. 12a) and 600-hPa relative humidity (Fig. 12b) are in good agreement with GPI anomalies at the different intraseasonal IPCO phases. This implies that these two factors may play a leading role in TC genesis compared to the other two factors. Much previous research has proved that smaller vertical wind shear favors the TC genesis (Goldenberg and Shapiro 1996, Maloney and Hartmann 2000a,b, Bessafi and Wheeler 2006). Also, the linear term is associated with the ISO of 200–850-hPa wind shear (Fig. 12c) is agreement with GPI anomalies in the NIO north of 13°N and most areas of the WNP, suggesting that vertical wind shear may play a considerable role in affecting TC genesis in different basins. However, the linear term associated with the ISO of potential intensity (Fig. 12d) even shows an opposite pattern with GPI anomalies at corresponding phase, suggesting potential intensity may play only a small role in regulating TC genesis.

6. Summary and discussion

In this paper, we discuss the effect of the intraseasonal IPCO on tropical cyclone (TC) genesis location and frequency over the Indo–WNP during the boreal extended summer and present possible physical mechanisms. For the intraseasonal IPCO, the average situations in 850-hPa horizontal wind or OLR anomalies are very similar to the ones in the BSISO in the boreal extended summer, but the largest variance of the intraseasonal IPCO in the propagation related to the BSISO does not exceed 40% in all phases. There are doubtless some similarities in the impact of IPCO and BSISO (Kikuchi and Wang 2010; Yoshida et al. 2014) on TC genesis, such as the similar average TC genesis locations in the positive and negative phases in

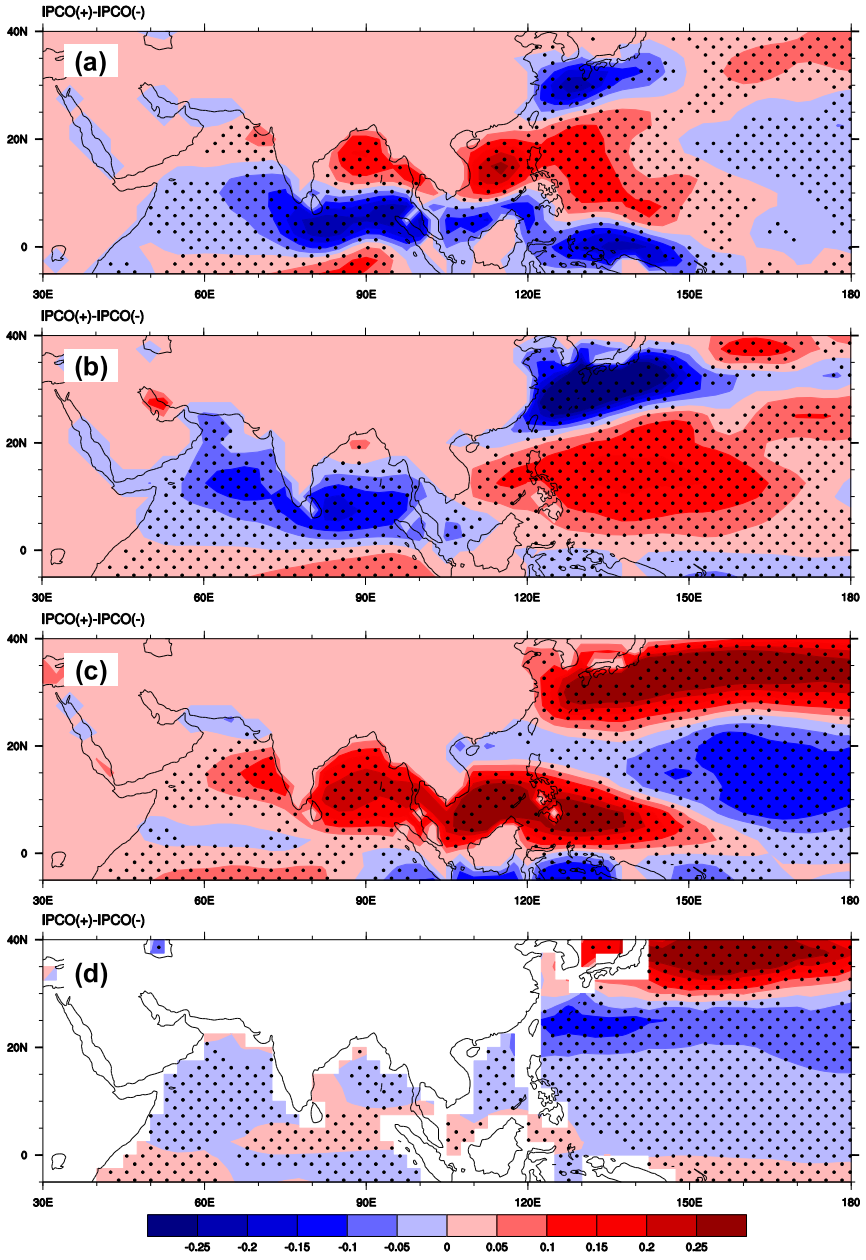

FIG. 12. As in Fig. 6, but for linear terms associated with the ISO of the GPI, including the (a) 850-hPa vorticity, (b) 600-hPa relative humidity, (c) 200–850-hPa wind shear, and (d) potential intensity.

the WNP. Differences are also evident; for instance, the difference in total number of TC geneses between active and inactive phases with IPCO is much larger than that with BSISO in the WNP, the effects of the intraseasonal IPCO on TC genesis in each phase are different from that of the BSISO in the NIO, and so on. More details will be given in a future paper. These differences can better verify that the intraseasonal IPCO is not essentially the same as the BSISO.

As discussed earlier, when the intraseasonal IPCO is in a positive phase, there tend to be many more TCs over the WNP, especially in the SCS, and they are mainly distributed over 5°–20°N. The reverse is true in the negative phase when tropical cyclogenesis is more widely dispersed and the TC genesis frequency is lower. In the NIO, there is no significant difference in the total number of TCs generated in the positive and negative intraseasonal IPCO phases. TC genesis mainly occurs

over 13°–20°N and closer to the Indian subcontinent in the positive intraseasonal IPCO phase, particularly in the ARB. In contrast, the distribution is more dispersed in the negative phase. In general, in the positive phase of the intraseasonal IPCO the distribution of TC genesis locations over the Indo–WNP is more concentrated, whereas in the negative phase it is more dispersed; this is referred to as the ''phase lock of TC genesis location.''

Possible physical mechanisms are also discussed in this study. In the WNP, when the intraseasonal IPCO is in a positive phase, the anomalous cyclonic circulation and the weakened WPSH provide circulation conditions favoring TC genesis. Latent heat release of cumulus convective condensation in the middle atmosphere contributes to the development and persistence of the TC warm core structure. This leads to more TC genesis in the positive phase. Meanwhile, with the shrinking of the WPSH and the westward shift of the center of anomalous cyclonic circulation, the distribution of TC genesis becomes locked to the west of the WNP and around 5°–20°N, and more TCs are generated in the SCS. The opposite situation occurs in the negative phase.

North of 13°N in the NIO, when the intraseasonal IPCO is in a positive phase, the increasing latent heat release of cumulus convective condensation, as well as the intensified anomalous cyclonic circulation, is centered on both sides of the Indian subcontinent, especially in the ARB. TCs form more readily in these regions. To the south of 13°N in the NIO, the latent heat release of cumulus convective condensation is suppressed, and an anomalous anticyclonic circulation is observed. These conditions suppress TC genesis. As such, there is no significant total frequency difference in the two phases. However, this asymmetry between conditions in the northern and southern NIO causes the difference in TC genesis locations in the positive and negative intraseasonal IPCO phases. The TC genesis locations have a northward shift (mainly to 13°–20°N) and lie closer to the Indian subcontinent in the positive phase, particularly in the ARB. In the negative phase, the opposite situation occurs.

Furthermore, we verify the importance of each linear term associated with the ISO of the GPI. The midlevel relative humidity and low-level vorticity are the two largest contributors to the TC genesis at different intraseasonal IPCO phases. Vertical wind shear is found to play considerable role in affecting TC genesis in different basins, and the role of potential intensity is small. These results are similar to previous studies (Camargo et al. 2007, 2009; Jiang et al. 2012; Zhao et al. 2015a,b), which further proves the present results' reliability. Also, the total contribution of linear terms can better express the westward distribution over the WNP than GPI anomalies. It needs to be noticed that these four linear terms cannot entirely represent the roles of the four factors (midlevel relative humidity, low-level vorticity, vertical wind shear, and potential intensity) because the GPI is a nonlinear combination of four parameters, and any change of one parameter could lead to change of action related to other parameters (Kikuchi and Wang 2010). Just like the role of vertical wind shear on TC genesis at different intraseasonal IPCO phases, the total nonlinear terms of GPI contribute differently in different basins.

The previous discussion suggests a close connection between TC activity and the intraseasonal IPCO. It is necessary that we need to take the change of convection activity, such as the intraseasonal IPCO, into consideration in TC forecasting. However, we have only considered the modulation by the intraseasonal IPCO of TC genesis location and frequency in the positive and negative intraseasonal IPCO phases over the Indo–WNP during the boreal extended summer in this paper. In fact, a series of more detailed investigations is required owing to the time sensitivity of the current results. TC genesis and development at intermediate phases of the intraseasonal IPCO will be pursued in future work.

Acknowledgments. Our sincere appreciation goes to Lidou Huyan, Zhaolu Hou, Quanjia Zhong, Jiaqing Xue, Yidan Xu, Yuehong Wang, Yazhou Zhang, and Di Dong for their valuable help. Also, we are grateful to NOAA for providing the latest OLR data (1979–2015). This work was jointly supported by the National Natural Science Foundation of China (NSFC; 41530424 and 41375110) and State Oceanic Administration (SOA) International Cooperation Program on Global Change and Air–Sea Interactions (GASI-IPOVAI-03). J. Zheng is funded by the NSFC project 41505074.

REFERENCES

Anthes, R. A., Ed., 1982: *Tropical Cyclones: Their Evolution, Structure, and Effects. Meteor. Monogr.*, No. 41, Amer. Meteor. Soc., 208 pp.

Bessafi, M., and M. C. Wheeler, 2006: Modulation of south Indian Ocean tropical cyclones by the Madden–Julian oscillation and convectively coupled equatorial waves. *Mon. Wea. Rev.*, **134**, 638–656, https://doi.org/10.1175/MWR3087.1.

Bister, M., and K. A. Emanuel, 2002a: Low frequency variability of tropical cyclone potential intensity. 1. Interannual to interdecadal variability. *J. Geophys. Res.*, **107**, 4801, https://doi.org/10.1029/2001JD000776.

——, and ——, 2002b: Low frequency variability of tropical cyclone potential intensity. 2. Climatology for 1982–1995. *J. Geophys. Res.*, **107**, 4621, https://doi.org/10.1029/2001JD000780.

Camargo, S. J., and A. H. Sobel, 2010: Revisiting the influence of the quasi-biennial oscillation on tropical cyclone activity. *J. Climate*, **23**, 5810–5825, https://doi.org/10.1175/2010JCLI3575.1.

——, K. A. Emanuel, and A. H. Sobel, 2007: Use of a genesis potential index to diagnose ENSO effects on tropical cyclone genesis. *J. Climate*, **20**, 4819–4834, https://doi.org/10.1175/JCLI4282.1.

——, M. C. Wheeler, and A. H. Sobel, 2009: Diagnosis of the MJO modulation of tropical cyclogenesis using an empirical index. *J. Atmos. Sci.*, **66**, 3061–3074, https://doi.org/10.1175/2009JAS3101.1.

Chan, J. C. L., 1995: Tropical cyclone activity in the western North Pacific in relation to the stratospheric quasi-biennial oscillation. *Mon. Wea. Rev.*, **123**, 2567–2571, https://doi.org/10.1175/1520-0493(1995)123<2567:TCAITW>2.0.CO;2.

——, 2000: Tropical cyclone activity over the western North Pacific associated with El Niño and La Niña events. *J. Climate*, **13**, 2960–2972, https://doi.org/10.1175/1520-0442(2000)013<2960:TCAOTW>2.0.CO;2.

Elsberry, R. L., and H.-C. Tsai, 2016: Opportunities and challenges in the dynamical and predictability studies of tropical cyclone events. *Dynamics and Predictability of Large-Scale, High-Impact Weather and Climate Events*, J. P. Li et al., Eds., Special Publications of the International Union of Geodesy and Geophysics Series, Vol. 2, Cambridge University Press, 133–140.

——, W. M. Frank, G. J. Holland, J. D. Jarrell, and R. L. Southern, 1987: *A Global View of Tropical Cyclones.* Office of Naval Research, 185 pp.

Emanuel, K. A., 1995: Sensitivity of tropical cyclones to surface exchange coefficients and a revised steady-state model incorporating eye dynamics. *J. Atmos. Sci.*, **52**, 3969–3976, https://doi.org/10.1175/1520-0469(1995)052<3969:SOTCTS>2.0.CO;2.

——, 2003: Tropical cyclones. *Annu. Rev. Earth Planet. Sci.*, **31**, 75–104, https://doi.org/10.1146/annurev.earth.31.100901.141259.

——, 2005: Increasing destructiveness of tropical cyclones over the past 30 years. *Nature*, **436**, 686–688, https://doi.org/10.1038/nature03906.

——, and D. S. Nolan, 2004: Tropical cyclone activity and global climate. *26th Conf. on Hurricanes and Tropical Meteorology*, Miami, FL, Amer. Meteor. Soc., 10A.2, https://ams.confex.com/ams/pdfpapers/75463.pdf.

Feng, T., X. Y. Shen, R. H. Huang, and G. H. Chen, 2014: Influence of the interannual variation of cross-equatorial flow on tropical cyclogenesis over the western North Pacific (in Chinese). *J. Trop. Meteor.*, **30**, 11–12.

Goldenberg, S. B., and L. J. Shapiro, 1996: Physical mechanisms for the association of El Niño and West African rainfall with Atlantic major hurricane activity. *J. Climate*, **9**, 1169–1187, https://doi.org/10.1175/1520-0442(1996)009<1169:PMFTAO>2.0.CO;2.

Gray, W. M., 1968: Global view of the origin of tropical disturbances and storms. *Mon. Wea. Rev.*, **96**, 669–700, https://doi.org/10.1175/1520-0493(1968)096<0669:GVOTOO>2.0.CO;2.

——, 1979: Hurricanes: Their formation, structure and likely role in the tropical circulation. *Meteorology over the Tropical Oceans*, D. B. Shaw, Ed., Royal Meteorological Society, 155–218.

Hack, J. J., and W. H. Schubert, 1986: Nonlinear response of atmospheric vortices to heating by organized cumulus convection. *J. Atmos. Sci.*, **43**, 1559–1573, https://doi.org/10.1175/1520-0469(1986)043<1559:NROAVT>2.0.CO;2.

Hartmann, D. L., and E. D. Maloney, 2001: The Madden–Julian oscillation, barotropic dynamics, and North Pacific tropical cyclone formation. Part II: Stochastic barotropic modeling. *J. Atmos. Sci.*, **58**, 2559–2570, https://doi.org/10.1175/1520-0469(2001)058<2559:TMJOBD>2.0.CO;2.

Ho, C.-H., J.-J. Baik, J.-H. Kim, D.-Y. Gong, and C.-H. Sui, 2004: Interdecadal changes in summertime typhoon tracks. *J. Climate*, **17**, 1767–1776, https://doi.org/10.1175/1520-0442(2004)017<1767:ICISTT>2.0.CO;2.

Holland, G. J., 1987: Mature structure and structure change. *A Global View of Tropical Cyclones*, R. L. Elsberry et al., Eds., Office of Naval Research, 13–52.

Holton, J. R., 2004: *An Introduction to Dynamic Meteorology.* 4th ed. Elsevier Academic Press, 540 pp.

Huang, P., C. Chou, and R. H. Huang, 2011: Seasonal modulation of tropical intraseasonal oscillations on tropical cyclone geneses in the western North Pacific. *J. Climate*, **24**, 6339–6352, https://doi.org/10.1175/2011JCLI4200.1.

Huo, L. W., P. W. Guo, S. N. Hameed, and D. C. Jin, 2015: The role of tropical Atlantic SST anomalies in modulating western North Pacific tropical cyclone genesis. *Geophys. Res. Lett.*, **42**, 2378–2384, https://doi.org/10.1002/2015GL063184.

Jiang, X., M. Zhao, and D. E. Waliser, 2012: Modulation of tropical cyclones over the eastern Pacific by the intraseasonal variability simulated in an AGCM. *J. Climate*, **25**, 6524–6538, https://doi.org/10.1175/JCLI-D-11-00531.1.

Kalnay, E., and Coauthors, 1996: The NCEP/NCAR 40-Year Reanalysis Project. *Bull. Amer. Meteor. Soc.*, **77**, 437–471, https://doi.org/10.1175/1520-0477(1996)077<0437:TNYRP>2.0.CO;2.

Kepert, J. D., 2010: Tropical cyclone structure and dynamics. *Global Perspectives on Tropical Cyclones: From Science to Mitigation*, J. C. L. Chan and J. D. Kepert, Eds., World Scientific Series on Asia-Pacific Weather and Climate, Vol. 4, World Scientific, 3–54.

Kikuchi, K., and B. Wang, 2010: Formation of tropical cyclones in the northern Indian Ocean associated with two types of intraseasonal oscillation modes. *J. Meteor. Soc. Japan*, **88**, 475–496, https://doi.org/10.2151/jmsj.2010-313.

——, ——, and Y. Kajikawa, 2012: Bimodal representation of the tropical intraseasonal oscillation. *Climate Dyn.*, **38**, 1989–2000, https://doi.org/10.1007/s00382-011-1159-1.

Kim, H.-M., P. J. Webster, and J. A. Curry, 2009: Impact of shifting patterns of Pacific Ocean warming on North Atlantic tropical cyclones. *Science*, **325**, 77–80, https://doi.org/10.1126/science.1174062.

Kim, J.-H., C.-H. Ho, H.-S. Kim, C.-H. Sui, and S. K. Park, 2008: Systematic variation of summertime tropical cyclone activity in the western North Pacific in relation to the Madden–Julian oscillation. *J. Climate*, **21**, 1171–1191, https://doi.org/10.1175/2007JCLI1493.1.

Knutson, T. R., and Coauthors, 2010: Tropical cyclones and climate change. *Nat. Geosci.*, **3**, 157–163, https://doi.org/10.1038/ngeo779.

Kossin, J. P., and D. J. Vimont, 2007: A more general framework for understanding Atlantic hurricane variability and trends. *Bull. Amer. Meteor. Soc.*, **88**, 1767–1781, https://doi.org/10.1175/BAMS-88-11-1767.

Lau, K.-M., and P. H. Chan, 1986: Aspects of the 40–50 day oscillation during the northern summer as inferred from outgoing longwave radiation. *Mon. Wea. Rev.*, **114**, 1354–1367, https://doi.org/10.1175/1520-0493(1986)114<1354:AOTDOD>2.0.CO;2.

Li, J. P., G. X. Wu, and D. X. Hu, 2011: *Ocean–Atmosphere Interaction over the Joining Area of Asia and Indian–Pacific*

Ocean and Its Impact on the Short-Term Climate Variation in China (in Chinese). Vol. 1, China Meteorological Press, 516 pp.

——, and Coauthors, 2013a: Progress in air–land–sea interactions in Asia and their role in global and Asian climate change (in Chinese). *Chin. J. Atmos. Sci.*, **37**, 518–538.

——, C. Sun, and F.-F. Jin, 2013b: NAO implicated as a predictor of Northern Hemisphere mean temperature multidecadal variability. *Geophys. Res. Lett.*, **40**, 5497–5502, https://doi.org/10.1002/2013GL057877.

——, R. Swinbank, R. Grotjahn, and H. Volkert, Eds., 2016a: *Dynamics and Predictability of Large-Scale, High-Impact Weather and Climate Events.* Special Publications of the International Union of Geodesy and Geophysics Series, Vol. 2, Cambridge University Press, 370 pp.

——, Q. Y. Wang, Y. J. Li, and J. W. Zhang, 2016b: Review and perspective on the climatological research of tropical cyclones in terms of energetics (in Chinese). *J. Beijing Norm. Univ. Nat. Sci.*, **52**, 705–713.

Li, R. C. Y., and W. Zhou, 2013a: Modulation of western North Pacific tropical cyclone activity by the ISO. Part I: Genesis and intensity. *J. Climate*, **26**, 2904–2918, https://doi.org/10.1175/JCLI-D-12-00210.1.

——, and ——, 2013b: Modulation of western North Pacific tropical cyclone activity by the ISO. Part II: Tracks and landfalls. *J. Climate*, **26**, 2919–2930, https://doi.org/10.1175/JCLI-D-12-00211.1.

Li, X. Z., 1956: A comprehensive theory for the typhoon genesis (in Chinese). *Acta Meteor. Sin.*, **27**, 87–89.

Li, Y., J. P. Li, and J. Feng, 2012: A teleconnection between the reduction of rainfall in southwest western Australia and north China. *J. Climate*, **25**, 8444–8461, https://doi.org/10.1175/JCLI-D-11-00613.1.

Li, Y. J., J. P. Li, and J. Feng, 2013: Boreal summer convection oscillation over the Indo-western Pacific and its relationship with the East Asian summer monsoon. *Atmos. Sci. Lett.*, **14**, 66–71, https://doi.org/10.1002/asl2.418.

Liebmann, B., and C. A. Smith, 1996: Description of a complete (interpolated) outgoing longwave radiation dataset. *Bull. Amer. Meteor. Soc.*, **77**, 1275–1277.

Liu, K. S., and J. C. L. Chan, 2008: Interdecadal variability of western North Pacific tropical cyclone tracks. *J. Climate*, **21**, 4464–4476, https://doi.org/10.1175/2008JCLI2207.1.

Lu, R. Y., 2001: Interannual variability of the summertime North Pacific subtropical high and its relation to atmospheric convection over the warm pool. *J. Meteor. Soc. Japan*, **79**, 771–783, https://doi.org/10.2151/jmsj.79.771.

Madden, R. A., 1986: Seasonal variations of the 40–50 day oscillation in the tropics. *J. Atmos. Sci.*, **43**, 3138–3158, https://doi.org/10.1175/1520-0469(1986)043<3138:SVOTDO>2.0.CO;2.

——, and P. R. Julian, 1972: Description of global-scale circulation cells in the tropics with a 40–50 day period. *J. Atmos. Sci.*, **29**, 1109–1123, https://doi.org/10.1175/1520-0469(1972)029<1109:DOGSCC>2.0.CO;2.

——, and ——, 1994: Observations of the 40–50-day tropical oscillation—A review. *Mon. Wea. Rev.*, **122**, 814–837, https://doi.org/10.1175/1520-0493(1994)122<0814:OOTDTO>2.0.CO;2.

Maloney, E. D., and D. L. Hartmann, 2000a: Modulation of eastern North Pacific hurricanes by the Madden–Julian oscillation. *J. Climate*, **13**, 1451–1460, https://doi.org/10.1175/1520-0442(2000)013<1451:MOENPH>2.0.CO;2.

——, and ——, 2000b: Modulation of hurricane activity in the Gulf of Mexico by the Madden–Julian oscillation. *Science*, **287**, 2002–2004, https://doi.org/10.1126/science.287.5460.2002.

Pyper, B. J., and R. M. Peterman, 1998: Comparison of methods to account for autocorrelation in correlation analyses of fish data. *Can. J. Fish. Aquat. Sci.*, **55**, 2127–2140, https://doi.org/10.1139/f98-104.

Sobel, A. H., and S. J. Camargo, 2005: Influence of western North Pacific tropical cyclones on their large-scale environment. *J. Atmos. Sci.*, **62**, 3396–3407, https://doi.org/10.1175/JAS3539.1.

Sun, C., J. P. Li, J. Feng, and F. Xie, 2015: A decadal-scale teleconnection between the North Atlantic Oscillation and subtropical eastern Australian rainfall. *J. Climate*, **28**, 1074–1092, https://doi.org/10.1175/JCLI-D-14-00372.1.

Wang, B., and J. C. L. Chan, 2002: How strong ENSO events affect tropical storm activity over the western North Pacific. *J. Climate*, **15**, 1643–1658, https://doi.org/10.1175/1520-0442(2002)015<1643:HSEEAT>2.0.CO;2.

——, and J.-Y. Moon, 2017: An anomalous genesis potential index for MJO modulation of tropical cyclones. *J. Climate*, **30**, 4021–4035, https://doi.org/10.1175/JCLI-D-16-0749.1.

Webster, P. J., G. J. Holland, J. A. Curry, and H.-R. Chang, 2005: Changes in tropical cyclone number, duration, and intensity in a warming environment. *Science*, **309**, 1844–1846, https://doi.org/10.1126/science.1116448.

Xie, F., J. P. Li, W. S. Tian, J. K. Zhang, and C. Sun, 2014: The relative impacts of El Niño Modoki, canonical El Niño, and QBO on tropical ozone changes since the 1980s. *Environ. Res. Lett.*, **9**, 064020, https://doi.org/10.1088/1748-9326/9/6/064020.

Xing, N., J. P. Li, and Y. K. Li, 2014: Response of the tropical atmosphere to isolated equatorially asymmetric heating (in Chinese). *Chin. J. Atmos. Sci.*, **38**, 1147–1158.

Yoshida, R., Y. Kajikawa, and H. Ishikawa, 2014: Impact of boreal summer intraseasonal oscillation on environment of tropical cyclone genesis over the western North Pacific. *SOLA*, **10**, 15–18, https://doi.org/10.2151/sola.2014-004.

Yu, J. H., T. Li, Z. M. Tan, and Z. W. Zhu, 2016: Effects of tropical North Atlantic SST on tropical cyclone genesis in the western North Pacific. *Climate Dyn.*, **46**, 865–877, https://doi.org/10.1007/s00382-015-2618-x.

Yumoto, M., and T. Matsuura, 2001: Interdecadal variability of tropical cyclone activity in the western North Pacific. *J. Meteor. Soc. Japan*, **79**, 23–35, https://doi.org/10.2151/jmsj.79.23.

Zhan, R. F., Y. Q. Wang, and X. T. Lei, 2011a: Contributions of ENSO and east Indian Ocean SSTA to the interannual variability of northwest Pacific tropical cyclone frequency. *J. Climate*, **24**, 509–521, https://doi.org/10.1175/2010JCLI3808.1.

——, ——, and C.-C. Wu, 2011b: Impact of SSTA in east Indian Ocean on the frequency of northwest Pacific tropical cyclones: A regional atmospheric model study. *J. Climate*, **24**, 6227–6242, https://doi.org/10.1175/JCLI-D-10-05014.1.

——, ——, and M. Wen, 2013: The SST gradient between the southwestern Pacific and the western Pacific warm pool: A new factor controlling the northwestern Pacific tropical cyclone genesis frequency. *J. Climate*, **26**, 2408–2415, https://doi.org/10.1175/JCLI-D-12-00798.1.

——, ——, and L. Tao, 2014: Intensified impact of east Indian Ocean SST anomaly on tropical cyclone genesis frequency over the western North Pacific. *J. Climate*, **27**, 8724–8739, https://doi.org/10.1175/JCLI-D-14-00119.1.

——, Y. H. Ding, L. G. Wu, and X. T. Lei, 2016: Role of ENSO in the interannual relationship between Tibetan Plateau winter

snow cover and northwest Pacific tropical cyclone genesis frequency. *Sci. China Earth Sci.*, **59**, 2009–2021, https://doi.org/10.1007/s11430-015-5559-y.

——, B. D. Chen, and Y. H. Ding, 2017: Impacts of SST anomalies in the Indian-Pacific basin on northwest Pacific tropical cyclone activities during three super El Niño years. *Chin. J. Oceanol. Limnol.*, https://doi.org/10.1007/s00343-018-6321-8, in press.

Zhang, J. W., J. P. Li, and Y. J. Li, 2015: Intraseasonal characteristics of the Indo–west Pacific convection oscillation (in Chinese). *Chin. J. Atmos. Sci.*, **39**, 221–234.

Zhao, H. K., X. Jiang, and L. Wu, 2015a: Modulation of northwest Pacific tropical cyclone genesis by the intraseasonal variability. *J. Meteor. Soc. Japan*, **93**, 81–97, https://doi.org/10.2151/jmsj.2015-006.

——, R. Yoshida, and G. B. Raga, 2015b: Impact of the Madden–Julian oscillation on western North Pacific tropical cyclogenesis associated with large-scale patterns. *J. Appl. Meteor. Climatol.*, **54**, 1413–1429, https://doi.org/10.1175/JAMC-D-14-0254.1.

Zhao, J. W., R. F. Zhan, Y. Q. Wang, and L. Tao, 2016: Intensified interannual relationship between tropical cyclone genesis frequency over the northwest Pacific and the SST gradient between the southwest Pacific and the western Pacific warm pool since the mid-1970s. *J. Climate*, **29**, 3811–3830, https://doi.org/10.1175/JCLI-D-15-0729.1.

Zhu, B. Z., and B. Wang, 1993: The 30–60-day convection seesaw between the tropical Indian and western Pacific Oceans. *J. Atmos. Sci.*, **50**, 184–199, https://doi.org/10.1175/1520-0469(1993)050<0184:TDCSBT>2.0.CO;2.

Zhu, C. W., T. Nakazawa, and J. P. Li, 2004: Modulation of tropical depression/cyclone over the Indian–western Pacific oceans by Madden–Julian oscillation (in Chinese). *Acta Meteor. Sin.*, **62**, 42–50.

Zhu, Q. G., J. R. Lin, S. W. Shou, and D. S. Tang, 2007: *Principles and Methods of Synoptic Meteorology* (in Chinese). China Meteorological Press, 649 pp.